Experiments on the rapid mechanical expansion of liquid ^{4}He through its superfluid transition

V. B. Efimov,[1,2] O. J. Griffiths,[2] P. C. Hendry,[2] G. V. Kolmakov,[1,2] P. V. E. McClintock,[2] and L. Skrbek[2,3]
[1]*Institute of Solid State Physics, RAS, Chernogolovka, Russia*
[2]*Department of Physics, Lancaster University, Lancaster LA1 4YB, United Kingdom*
[3]*Joint Low Temperature Laboratory, Institute of Physics ASCR and Faculty of Mathematics and Physics, Charles University, V Holešovičkách 2, 180 00 Prague, Czech Republic*
(Received 21 June 2006; published 16 November 2006)

Phenomena following a rapid mechanical quench of liquid ^{4}He from its normal to its superfluid phase are reported and discussed. The mechanical expansion apparatus is an improved version of that described previously. It uses a double-cell geometry to effect a partial separation of the sample from the convolutions of the bellows that form the outer wall of the cell. Consistent with earlier work, no evidence is found for the production of quantized vortices via the Kibble-Zurek (KZ) mechanism. Although the expansion is complete within 15 ms, the second-sound velocity and attenuation continue to increase for a further ~60 ms; correspondingly the temperature decreases. Subsequently, the temperature rises again toward its final value as the second-sound velocity and attenuation decrease. It is shown that this unexpected behavior is apparently associated with a large-amplitude second-sound oscillation produced by the expansion, and it is suggested that the observed vortices are created by the normal fluid–superfluid counterflow that constitutes the second-sound wave. If production of large-amplitude second sound is inherent to the mechanical expansion of liquid ^{4}He through the superfluid transition, as appears to be the case for final temperatures more than 3 mK from the λ transition, the phenomenon sets a lower bound on the density of KZ vortices that can be detected in this type of experiment.

DOI: 10.1103/PhysRevE.74.056305 PACS number(s): 47.32.−y, 67.40.Vs, 67.55.Cx, 67.40.Pm

I. INTRODUCTION

The work reported below has grown from our attempts to improve on earlier experiments [1] designed to model the grand unification theory (GUT) symmetry-breaking phase transition of the early Universe by investigation of fast quenches of liquid ^{4}He from its normal to its superfluid state. At the GUT transition, the original symmetry of the Universe was lost: the vacuum entered a state of spontaneously broken symmetry and, correspondingly, the forces of nature separated. The transition is believed to have been of second order and to have occurred $\sim 10^{-35}$ s after the Big Bang, as the Universe fell through a critical temperature of $\sim 10^{27}$ K.

Near a second-order transition, the potential contribution V to the free-energy density can be approximated by

$$V = \alpha|\psi|^2 + \frac{1}{2}\beta|\psi|^4 \tag{1}$$

where $\alpha = \alpha(T - T_\lambda)$ with $\alpha > 0$. Thus α is positive above the transition and negative below it. A variety of topological defects is believed to have been created in the transition [2], including point defects, corresponding to magnetic monopoles; surface defects, called domain walls; and, of particular interest, stringlike defects, called cosmic strings. Cosmic string will be able to form when the order parameter (Higgs field) ψ is complex. In the broken-symmetry phase α is negative and $V(\psi)$ takes the shape of a sombrero hat.

Liquid ^{4}He undergoes a comparable second-order transition into its superfluid state at $T_\lambda \simeq 2$ K. The potential contribution to the free energy can be written in the same fashion (using the Ginzburg-Landau free energy equation [3]). Quantized vortices in superfluid helium are thus the analog of cosmic strings in cosmology [4] and the mechanism responsible for the creation of topological defects in the early Universe can in principle be modeled in the laboratory through a fast transition of liquid ^{4}He into its superfluid phase. The main aim of these experiments is to effect a fast passage of a small sample of liquid ^{4}He through the superfluid transition, and then to seek evidence of quantized vortices created in the quench. The vortices correspond to metastable excited states of the superfluid, so their density is expected to decrease rapidly following the quench.

The first experiment of this kind [5] yielded evidence of vortex creation, but subsequent investigations using an experimental cell of improved design [1] showed that vortices were not created at measurable densities; in fact, the upper limit on the density was more than two orders of magnitude below the theoretical expectation [6]. The analogous experiment on ^{3}He [7], however, provided evidence of vortex production at about the expected density. Likewise, the results of experiments on liquid crystals [8,9] and on superconductors [10,11] appear to be consistent with predictions based on the Kibble-Zurek (KZ) scenario [2,4].

The present project was undertaken to try to clarify the seemingly anomalous position of ^{4}He and, in particular, to reduce still further the upper bound on the initial density of KZ vortices. We also had in mind, however, that the normal-superfluid transition in liquid helium ^{4}He is an accessible and very interesting example of a second-order phase transition. By studying it, we can seek information about the associated critical fluctuations as well as—in principle—defect creation. We might thus hope to check our understanding of the two-fluid model of He II under critical conditions, as well as investigating vortex creation at the transition and the subsequent evolution of the vortex tangle. As we will see, however, the results obtained differ from expectation. They dem-

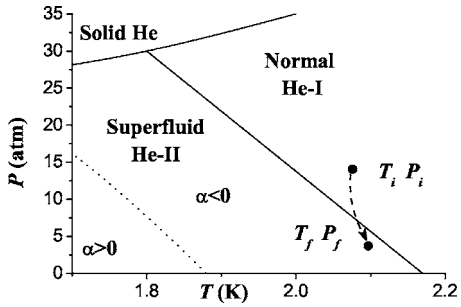

FIG. 1. Phase diagram of ^{4}He showing schematically (dashed line) a trajectory from an initial temperature and pressure (T_i, P_i) in He I to a final state (T_f, P_f) in He II. The dotted line separates regions of positive and negative nonlinear coefficients of second-sound velocity.

onstrate the existence of an additional vortex creation mechanism, perhaps inherent to expansion experiments of this kind, that would obscure the possible production of KZ vortices at a low density.

II. EXPERIMENTAL DETAILS

A quick transition of liquid helium from its normal phase (He I) into its superfluid one (He II) by cooling is impossible, given the logarithmic infinity in its heat capacity at T_λ. The experiment therefore moves the liquid into its superfluid phase by a rapid expansion. The phase diagram of ^{4}He allows such an adiabatic transition because T_λ is weakly pressure dependent (Fig. 1). The compressed, thermally isolated, small volume of He I (at pressure P_i and temperature T_i) is allowed to expand freely to a final point where it has become He II (at P_f and T_f). Zurek's original estimate of the vortex density (in cm^{-2}) created in the expansion was

$$L_i = \frac{1.2 \times 10^8}{(\tau_Q/100)^{2/3}} \tag{2}$$

where the quench time τ_Q is in milliseconds. To maximize the opportunity of observing KZ vortices, one should therefore try to minimize τ_Q. The main experimental problems lie in the speed of the process, which can be enhanced by minimizing the mass of the components moving during the expansion; the short distance T_f from T_λ, which can lead to difficulties including internal fluid fluxes caused by nonidealities of the expansion process; the mechanical shock of the expansion, which leads to vibration, noise in the electronics, and a "dead period" immediately following the expansion during which no measurements can be made.

Compared to our first- [5] and second- [1] generation versions of the expansion apparatus, the present cell differs in four important respects.

(1) To reduce the original dead period of ~50 ms, provision was made for damping out vibrations and oscillations. The reconstructed measuring cell allowed us to get information about possible vortices after about 10–15 ms.

(2) A different method was used to minimize flow caused by nonidealities in the expansion. Rather than using a very short cell as in [1] a longer cell with bellows was employed, similar to that in [5], but an *inner cell* was used to protect the measurement region from possible vortices generated hydrodynamically by the convolutions of the bellows.

(3) The modified geometry of the inner cell of our experimental chamber created good conditions for the study of relatively high-amplitude second-sound waves. In particular, its cylindrical construction allowed us to study wave attenuation in an effectively one-dimensional geometry, where the damping arises mainly from processes that occur within the bulk helium.

(4) More sensitive bolometry was employed, in which the resistive carbon paper of [5,1] was replaced with a Cu-Sn superconducting bolometer [12] biased to the middle of its transition by a magnetic field.

We now discuss the experimental arrangememts in more detail.

The expansion chamber is illustrated in Fig. 2. Its walls were formed from phosphor-bronze concertina bellows. It was filled with isotopically pure ^{4}He through a capillary tube, and then sealed with a needle valve. The top of the chamber was fixed rigidly to the cryostat but its bottom surface could be moved to compress the liquid, or released to expand it, using a pull rod from the top of the cryostat. The chamber was suspended in vacuum, surrounded by a reservoir of liquid ^{4}He at about 2 K. A capacitance gauge recorded the pressure in the chamber and carbon resistance thermometers were used to measure the temperatures in the reservoir and on the outside of the chamber.

A trigger mechanism on the mechanical linkage released the pull rod, allowing the cell to increase its volume by ~20% rapidly under its own initial internal pressure. A typical time dependence of the length of the bellows is plotted in Fig. 3. After completion of the expansion, the time taken for the chamber oscillations to subside was ~5 ms.

As in the earlier work [1,5], second-sound attenuation was used as the tool for quantifying the vortex line density L. The inner cell took the form of a quartz cylinder of diameter D =15 mm, length L_c=3 mm, with slots in its sides to maintain the same constant pressure inside and outside the cell; the expectation was that vortices produced at the convolutions, and any vortices created by outflow through the slots during the quench, would remain in the outer part of the cell on the time scale of the measurements. A meander film heater and a superconducting film bolometer were positioned on the top and bottom of the cylinder respectively. This inner cell was embedded within the expansion chamber, as shown in Fig. 2(c).

The superconducting transition temperature of the film bolometer [12] was adjusted by means of an external magnetic field. Its sensitivity of ~10 V/K then allowed temperature changes in the second-sound wave amplitude to be measured to better than 1 μK. The distance from T_λ was deduced from the second-sound velocity, determined from the transit time of the first reflected pulse.

The vortex density in the He II following the expansion was measured by recording the attenuation of a sequence of second-sound pulses propagated through the superfluid helium. An important feature of our present experimental cell is that it provides excellent conditions for probe wave propagation. The reason is connected to the marked differences be-

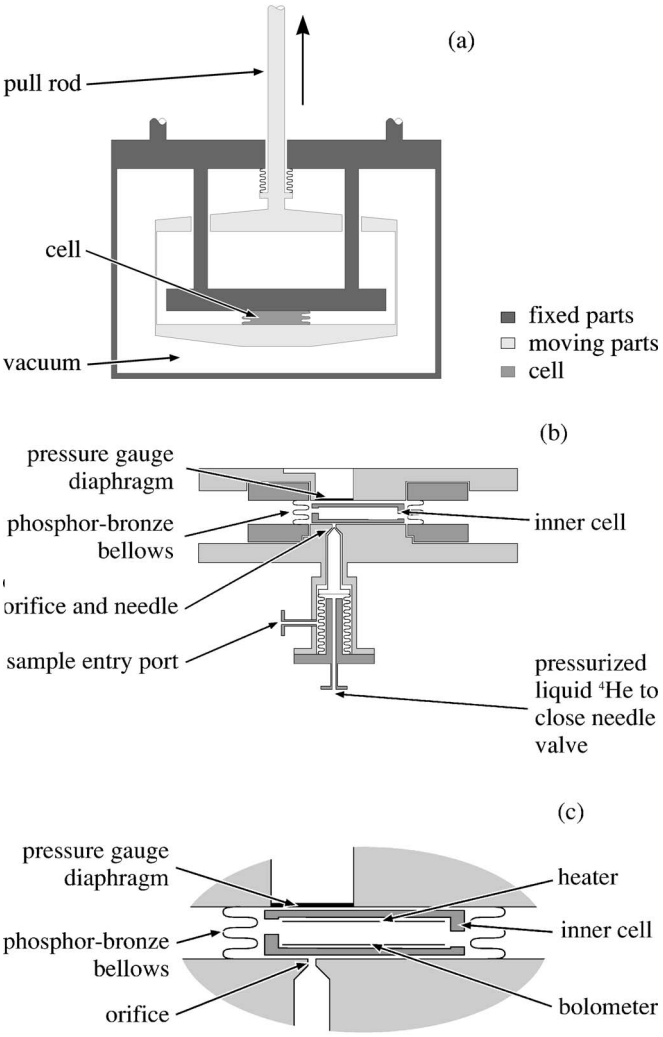

FIG. 2. Schematic diagrams of the expansion apparatus showing (a) the arrangements for filling and compressing the cell; (b) the outer cell; (c) the inner cell. The cylindrical cell was of quartz, closed by two plates holding the heater and bolometer, respectively. It was placed inside the expansion chamber, which had phosphor-bronze concertina walls. Slots in the cell walls allowed for equalization of the internal and external pressures. The sample filling capillary was closed off by means of a hydraulically operated needle valve after the chamber had been pressurized. A capacitance gauge was used to determine the pressure.

tween second-sound pulse propagation in one-dimensional (1D) and three-dimensional (3D) geometries.

Where the distance between the heater and bolometer (or the net distance after allowing for reflections) exceeds the linear size of the heater, the wave evolves as though in a 3D geometry. For first (i.e., ordinary) sound the pulse shape of the probe signal then transforms, with a rarefaction wave following a wave of compression [13]; in the case of second sound, the heat pulse transforms into a heating-cooling pair [14–17]. The quench experiments are necessarily conducted near the normal-superfluid transition, where the second-sound nonlinearity coefficient α_2 is large and negative (approaching $-\infty$ as $T \rightarrow T_\lambda$). The heating-cooling pair produced in a three-dimensional geometry consequently tends to create

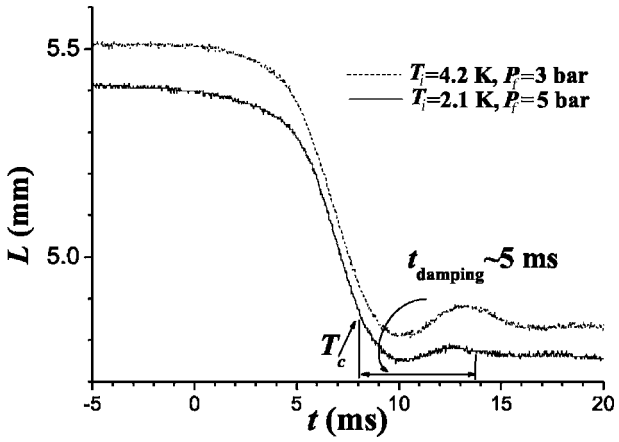

FIG. 3. Time dependence of the chamber length during typical expansions: from T_i=4.2 K, P_f=3 bar (top curve) ending in He I; and from T_i=2.1 K, P_f=4 bar (lower curve).

breakdown conditions at its center, resulting in a decrease in amplitude that has no connection with the vortices that the test pulse is intended to probe.

In the 1D case, however, a second-sound wave at temperature near T_λ in a medium with dissipation can be described by the nonlinear Burger's equation

$$u_t + (u_{20} + \alpha_2 u)u_x = \nu u_{xx} \tag{3}$$

where u_{20} is the second-sound velocity of vanishing amplitude wave and ν is the coefficient of wave damping in media. Because α_2 close to T_λ is so large and negative, a rectangular heat pulse transforms into a triangular temperature one at a short distance from the heater. Its width increases as it propagates, with a corresponding decrease in amplitude (Fig. 4). Thus a diminution of the energy of the propagating pulse (i.e., its *area* $Q=\int A dt$, not its amplitude) provides a measure of the vortex line density L in the liquid traversed by the pulse.

In our experiments we used a sequence of relatively infrequent rectangular probe pulses of length ~10 μs. Their repetition interval was in the range 10–50 ms. In each case, we recorded a sequence of reflected second-sound signals. Then we calculated the average ratio Q_{i+1}/Q_i for the first few

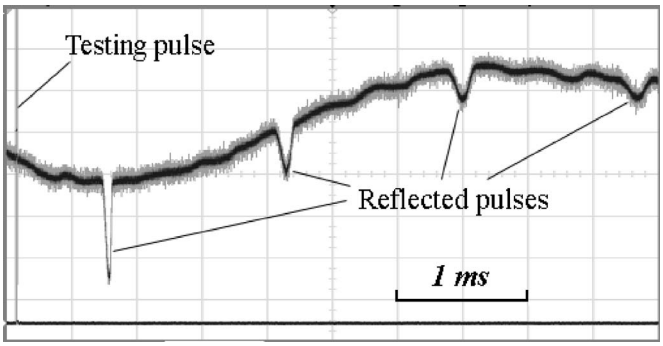

FIG. 4. Typical train of reflected second-sound pulses as detected by the bolometer, becoming more attenuated on successive passages through the vortex tangle. Note that the test pulses are superimposed on top of a slow oscillatory temperature oscillation.

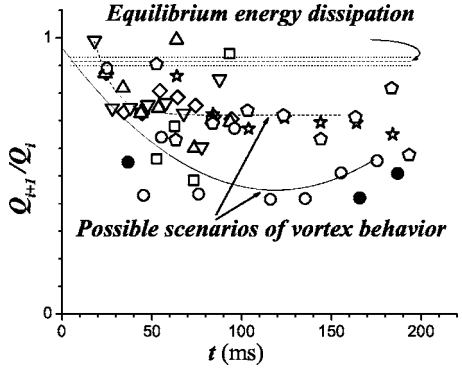

FIG. 5. Energy attenuation of successive second reflections, plotted as a function of time after the quench, providing a measure of the inverse vortex density. The relative attenuation in the absence of vortices is shown by the horizontal line at $Q_{i+1}/Q_i=0.9$.

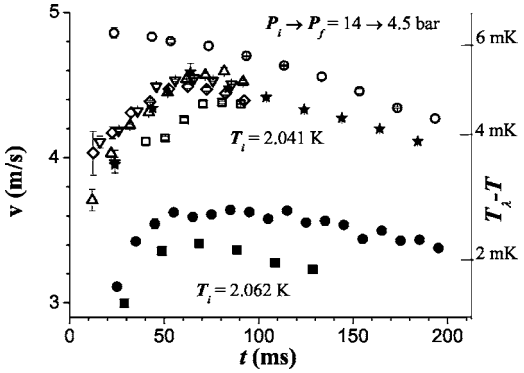

FIG. 6. Time dependence of the second-sound velocity $v(t,T)$ (left hand scale) after the quench for different initial temperatures T_i. The right hand scale shows the temperature difference from the superfluid transition, $T_\lambda - T$.

reflected pulses as a function of time (the average time elapsed since the superfluid transition was passed during the expansion). Their attenuation is of course determined by the sum of the attenuation on reflection (including geometrical effects) and the bulk dissipation due to vortices (the intrinsic bulk dissipation in the absence of vortices being negligible). We estimated the equilibrium energy dissipation on reflection experimentally from a sequence of reflected pulses at the same temperature T_f and pressure P_f as were reached in an expansion, but in the absence of the expansion: the attenuation during a path taking in a double reflection (bolometer-heater-bolometer) was less than 5%.

III. EXPERIMENTAL RESULTS

Our second-sound attenuation results following a quench are plotted in Fig. 5. Each point represents the averaged energy ratio Q_{i+1}/Q_i for a sequence of reflected pulses over a period of a few milliseconds, and is plotted at the average propagation time. In carrying out this procedure, we recorded at least three (rarely more than five) reflected signals. Despite the scatter of the data, it is evident that bulk dissipation of energy following a transition into the superfluid state is much higher than under equilibrium conditions (horizontal line). Furthermore, the dissipation clearly *increases* at first following the quench. The implication is that the vortex density also increases at first, in marked contrast to the originally expected evolution, which would be a monotonic decrease in attenuation if a tangle of Kibble-Zurek vortices had been created during the quench itself and was decaying away.

Figure 6 plots the evolution of the second-sound velocity (left-hand ordinate) and corresponding distance from T_λ (right-hand ordinate) following a quench. The same symbols are used in Figs. 5 and 6 for data obtained from a particular expansion. The open and filled symbols correspond to two sets of quenches with different initial and final conditions. It is evident that, with the exception of the data plotted as open circles, the velocity v and distance from T_λ at first increase, and then start to decrease again, with the two stages corresponding approximately in time to the two stages of second-sound attenuation shown in Fig. 5.

IV. DISCUSSION

A. Evolution of vortex density and temperature

The relationship between vortex density L and second-sound amplitude (here energy) $S=S_0\exp(-\eta x)$ may be written as [18]

$$L = \frac{6u_2 \ln(Q_i/Q_{i+1})}{\kappa B x} \tag{4}$$

where $\kappa=h/m_4=9.98\times10^{-4}$ cm^2 s^{-1} is the quantum of circulation, u_2 is the second-sound velocity, x is the distance over which the signal decreases from Q_i to Q_{i+1}, and the numerical constant $B\sim2-5$ was taken from earlier experiments on rotating helium. We estimate the maximum vortex line density from the energy dissipation $Q_{i+1}/Q_i\sim0.5$ as $\sim10^6$ cm^{-2}. If we suppose that there is a one-to-one relationship between the attenuation of the second-sound probe pulses and the vortex density within the cell, we must conclude that the vortex system after an expansion evolves through two distinct stages: (1) Immediately after the expansion there is a low (or zero) vortex line density L, which increases during the first ~100 ms, reaching a value of $\sim10^6$ cm^{-2}; and (2) the vortex tangle then decays.

As a consistency check, we can also estimate the vortex density attained in another way. In every experiment we observed a relatively slow temperature oscillation after the quench (see Fig. 7), which decayed over ~20 ms. We return later to consider its possible origins. The propagation of a harmonic wave through a vortex tangle may [19] be described as

$$\delta T = F(\zeta)e^{-\rho K t/2} \tag{5}$$

where $x=\zeta$ for $t=0$, and $F(x)$ gives the initial temperature disturbance. In the present case, the oscillation deviates from harmonic but we suppose the same picture applies to a good approximation. The amplitude of the oscillation decreases exponentially as $\exp(-\rho K t/2)$, due to mutual friction, with characteristic time $\rho K\simeq2\times10^{-2}$ s. The coefficient K can [20] be written as

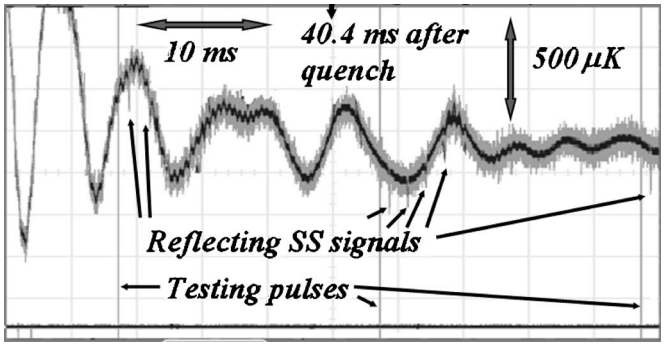

FIG. 7. Temperature oscillation in the cell after a quench. Vertical lines indicate the times when probe pulses were excited from the heater. The direct signal picked up by the bolometer, and some reflections, are indicated in each case. SS indicates second sound.

$$K = \frac{B}{3\rho}\kappa L \tag{6}$$

and we can ask whether or not the corresponding L is consistent with that calculated from Eq. (4). Accordingly, we can substitute the characteristic decay constant of the sine wave in Fig. 7. When we do so, we obtain a vortex line density $L \sim 10^6$ cm^{-2}, which represents reassuring consistency.

The mechanism responsible for the decay of a tangle of vortex lines is well-understood for the case when, as here, there is significant normal fluid density. The self-driven motion of the vortex cores through the viscous normal fluid is dissipative, resulting in line shrinkage, a process that is strongly amplified by the appearance of sharp cusps produced where lines have reconnected [21,22]. It is the first stage of the evolution, with an *increasing* vortex density, that was for us unexpected and requires an explanation. We note immediately that the epoch during which the vortex line density is increasing vastly exceeds the expected creation time for KZ vortices during the expansion (which are expected to appear spontaneously at the superfluid transition).

So the question arises: If these vortices are not created in the expansion itself, where do they come from, and why does their line density continue to increase long after completion of the quench?

A possible clue as to what else may be going on in the liquid can be seen in the slow oscillatory background temperature level of the signal in Fig. 4; for clarity it is shown again on an extended timescale in Fig. 7. Very similar behavior was observed in both of the earlier chambers [1,5]. The oscillation period is of the order of the second-sound propagation time across the cell, ~5 ms. For comparison, the periods of longitudinal oscillations in the 1 m rod ($\sim 2 \times 1/5000 = 0.4$ ms), and that of pressure relaxation inside the ~2 cm diameter chamber ($\sim 2 \times 0.02/200 = 0.2$ ms) are considerably shorter. We calculated the average period of the temperature oscillation τ_T and determined its dependence on the second-sound velocity. From two set of quenches with different beginning and finishing points (Fig. 6), the results were $\tau_T = 4.94 \pm 0.52$ ms for $u_2 = 3.2$ m s^{-1} and $\tau_T = 4.12 \pm 0.91$ ms for $u_2 = 4.4$ m s^{-1}, which correspond to wavelengths of 18 and 17 mm, respectively. These are comparable with the dimensions of our cell. Such a temperature wave could correspond to nonequilibrium internal counterflows of the normal and superfluid components after expansion: in effect a decaying second-sound standing wave of large amplitude.

B. Vortex dynamics

We hypothesize that, as in the case of pulsed second sound [23], the superfluid–normal fluid counterflow velocity in the standing wave may be sufficient to cause growth of vortices that are initially present following the expansion. It is highly likely that the liquid will contain such vortex "seeds:" there will presumably be the usual remanent vortex lines [24] that are believed to exist in all samples of He II, however prepared; added to which there may be vortices created via the Kibble-Zurek mechanism, albeit at an undetectably low density. Would the normal fluid–superfluid counterflow involved in the second-sound standing wave be likely to increase this initial vortex density?

Immediately after the quench, the amplitude of the temperature oscillations is ~0.5 mK when the liquid is ~5 mK below T_λ. This corresponding counterflow velocity of [25] $w = |\bar{v}_n - \bar{v}_s|$ is defined by

$$\delta T = \frac{u_2 \rho_n}{S} |\bar{v}_n - \bar{v}_s| \tag{7}$$

which yields $w \sim 17$ cm s^{-1}. Because $v_s = (\rho_n/\rho_s) \times v_n$, the normal component remains almost immobile. This counterflow velocity would indeed be sufficient to cause vortex growth, generating a tangle as described by the Hall-Vinen equation [26,27]

$$\frac{dL}{dt} = \alpha w L^{3/2} - \beta L^2. \tag{8}$$

Here α and β are Hall-Vinen constants, which have been extracted from experiments with heat pulse propagation [23]. The latter were conducted at temperatures far from T_λ ($T = 1.4$ to 1.85 K). They resulted in the formation of a vortex density of $L \sim 10^7$ cm^{-2} for $w \approx 40$ cm s^{-1} during a time span of 10 ms, corresponding to the equilibrium density

$$L_0 = \left(\frac{\alpha w}{\beta}\right)^2. \tag{9}$$

Extrapolating the data of [23] to near T_λ we find $\gamma = \alpha/\beta \sim 200$ s cm^{-2} which, taken with the above value of $w \sim 17$ cm s^{-1}, yields $L_0 \sim 10^7$ cm^{-2}. This is considerably larger than our above estimate of $\sim 10^6$ cm^{-2} based on the experiments. The most probable reason lies in the complex changes in vortex behavior that take place near T_λ.

The force acting on a unit length of a vortex can be written as

$$\mathbf{f} = \rho_s \kappa \times (v_L - v_s) - \eta \kappa \times [\kappa \times (v_n - v_L)] + \eta' \kappa \times (v_n - v_L). \tag{10}$$

Here the indices L, n, and s refer to the velocities of the vortex line and normal and superfluid components, respec-

tively, and κ stands for the circulation quantum (where repeated within a term, the additional one stands for a unit vector in the direction of κ). The first term on the right-hand side is the Magnus force, and the second and third terms are, respectively, the dissipative and nondissipative mutual friction forces.

In He II at low temperature both the dissipative (η) and nondissipative (η') mutual friction coefficients are negligibly small and vortex lines move with the superfluid velocity (and also due to the curvature of the line, which is not considered here as for simplicity we assume the vortex line to be straight).

It is relevant and interesting to consider the equivalent situation in ^{3}He-B, where the highly viscous normal component is effectively clamped by the walls in a container of conventional laboratory dimensions. Quantized vortices in the flow can be thought of as arranged in such a way that the coarse-grained hydrodynamic equation

$$\frac{\partial \mathbf{v}_s}{\partial t} + \nabla \mu = (1 - \eta')\mathbf{v}_s \times \boldsymbol{\omega} + \eta \hat{\boldsymbol{\omega}} \times (\boldsymbol{\omega} \times \mathbf{v}_s) \qquad (11)$$

obtained from the Euler equation after averaging over vortex lines [28], written in the frame of reference of the normal fluid, provides a sufficiently accurate description of the superflow. The normal fluid thus provides a unique frame of reference (at rest in the laboratory frame) and we have to deal only with the superfluid velocity $\mathbf{v}$. By rescaling the time such that $\tilde{t}=(1-\eta' t)$, and then dropping the tilde, one gets [29]

$$\frac{\partial \mathbf{v}}{\partial t} + \nabla \mu = \mathbf{v} \times \boldsymbol{\omega} + q \hat{\boldsymbol{\omega}} \times (\boldsymbol{\omega} \times \mathbf{v}) \qquad (12)$$

where ω denotes the (superfluid) vorticity and the important parameter $q=\eta/(1-\eta')$. Values of η and η' in ^{3}He are given in [30]. It has been shown that this equation (written in the continuous approximation) describes the dynamics of vortex motion in that when $q \gg 1$ the dynamics is "regular," while when $q \ll 1$, nonlinear multiplication of vortices may take place leading to the generation of a vortex tangle, i.e., superfluid turbulence. The experiment [31] showed a crossover between those two regimes as a function of T only at $T/T_c \approx 0.6$, where q is about 1.

In He II, however, the kinematic viscosity of the normal fluid is very low: the normal fluid moves easily and therefore does not provide the necessary unique reference frame, stationary in the laboratory. We plot the dimensionless quantity q versus temperature in Fig. 8, using tabulated values of $\eta(T)$ and $\eta'(T)$ from [32]. In He II q becomes of order 1 close to T_λ, approximately 5 mK below the transition. So the expansion trajectories terminate just in the region where the crossover occurs. We conclude the following.

(1) Far below T_λ, where $q<1$, the vortex density can be magnified by normal fluid–superfluid counterflow according to Eq. (8) (corresponding to the range $T/T_c<0.6$ in the case of superfluid ^{3}He).

(2) At temperatures close to T_λ, where $q>1$ (say, at $T_\lambda - T<2$ mK), the vortex system is overdamped, so that there is no vortex amplification even for large w (corresponding to the range $T/T_c>0.6$ in the case of superfluid ^{3}He).

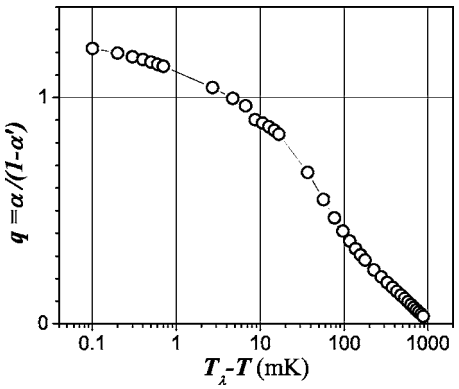

FIG. 8. The parameter $q=\alpha/(1-\alpha')$ (dimensionless units) plotted versus $T_\lambda - T$ for He II.

(3) In the temperature region of our experiments, where $q \sim 1$, the vortex density may increase, but to a smaller extent than predicted by (9).

Note that a similar deviation of measured from theoretical values was observed in [23].

It must be emphasized that the above estimates are approximate. Additional factors to those already mentioned are that a heat flux is known to cause a decrease [33] in T_λ and that, for a sufficient heat flux, the superfluidity may become thermodynamically unstable [34,35]. Nonetheless, it appears that production of vorticity in the second-sound oscillation following the expansion is the most likely explanation of the experimental results of Fig. 5.

C. Use of expansion experiments for modeling the KZ scenario

If the observed second-sound oscillation is inherent to expansion experiments of the kind discussed here, then it must set a limit on the KZ vortex line density that can be measured in this way. The empirical evidence, based on three expansion cells of different design (see above), is that such an oscillation always follows the expansion. Where does it come from?

Up to now we have supposed that the liquid in the cell expands uniformly, but of course this assumption represents an approximation. In reality, the expansion must be accompanied by gradients of pressure and temperature. When the bottom plate of the chamber (mass $\sim$1 kg; see Fig. 2) is released, it begins to accelerate under a force $\sim$200 N. The changing pressure propagates across the chamber ($\sim$5 mm) at the velocity of first sound. Consequently, the superfluid transition near the plate occurs $\sim$25 μs earlier than it does on the other side of chamber, and there must be corresponding gradients in the normal and superfluid densities of concentration, ρ_n and ρ_s. The expansion over a distance of $\sim$1 mm takes place in a characteristic time $\tau \sim 3$ ms, and the final velocity reached by the plate is $v_0 \sim 0.6$ m/s. The expansion is then stopped almost discontinuously by an attachment on the pull rod hitting a room-temperature stop. This sudden termination of the motion of the plate must generate

a return wave of pressure, temperature, and normal and superfluid concentrations.

The amplitude of the velocity oscillations in a liquid in the first sound wave created by movement of a container wall is proportional to the second-order time derivative of the velocity of the wall (cf. the result obtained for conventional sound generated by a moving body immersed into a compressible liquid [13]). Estimations for a one-dimensional sound wave excited in a container of length L during the expansion yield

$$v_n \approx v_s \sim \frac{L^2}{u_1^2}\frac{d^2v}{dt^2} \sim \frac{L^2 v_0}{u_1^2 \tau^2},$$

where v is the velocity of the moving wall and u_1 is the velocity of first sound. The temperature oscillations in such a first sound wave [25] are

$$\delta T_1 = -\frac{\rho \beta T u_1 v_s}{C}$$

where C is the heat capacity per unit mass of liquid helium, ρ is its density, and $\beta = -(1/\rho)(\partial\rho/\partial T)$ is the thermal expansion coefficient. For $T_\lambda - T = 3$ mK and at saturated vapor pressure one obtains $\delta T_1 < 1$ μK, which would be beneath the resolution of our superconducting bolometer. Similar estimation of the amplitude of second sound wave created in the expansion process gives (σ is the entropy per unit mass of liquid helium)

$$\delta T_2 = \frac{\beta \rho u_2^3 v_0}{\rho_s \sigma^2} \sim 4\mu\mathrm{K}.$$

Second sound therefore appears to provide the dominant temperature oscillation caused by a moving wall in He II, but the effect seems to be of much smaller amplitude than the oscillation seen in the experiments.

There exist, however, factors not so far considered that could lead to huge increases in the amplitudes of both first and sound under the conditions considered. During a fast transition of liquid ^{4}He from the normal to the superfluid state the $\beta(T,P)$ coefficient passes through a singularity at temperatures slightly above the λ line, at $T - T_\lambda = 3-6$ mK depending on pressure P in a liquid: the absolute value of the coefficient is increased by a factor of 10^2-10^3 near the singularity [36]. In our case, the system must inevitably pass through this singularity during its expansion. It could very well cause the increase in the amplitudes of the waves by a factor $\sim 10^2$, which gives for the values of the amplitudes of the of first- and second-sound waves after the expansion $\delta T_1 \sim \delta T_2 \sim 0.1$ mK, as observed. We note in passing that, in earlier experiments, it was the increase in the thermal expansion of liquid helium near the λ line at elevated pressures that allowed bolometric detection of the temperature oscillations in the linear *first*-sound waves of rarefaction (heating) created by a heater in superfluid helium at low heat loads, and its transformation into a first-sound wave of cooling (compression) at high heat loads [37].

Gradients in the superfluid state, and normal-superfluid counterflow, are clearly inherent to expansion experiments on the second-order transition in ^{4}He. We have seen that the end point of the expansion currently lies in a crossover region of the phase diagram where vortices may to some extent be expanded by superfluid-normal counterflow. For ^{4}He under its saturated vapor pressure, the parameter $q=1$ at $T_\lambda - T = 3$ mK, and we would not anticipate that raising the pressure would change this number drastically. It is possible that restriction of the final temperature of the quench to lie within 1 mK of T_λ would allow measurement of the vortex line density created at the quench itself, without the ambiguity introduced by subsequent vortex amplification in the counterflow. If the scatter of the data (Fig. 5) can be reduced, a set of quench experiments with finishing points at different distances from T_λ could therefore provide an interesting way of studying the behavior of the vortex system.

V. CONCLUSIONS

Improvements of experimental technique and cell geometry have allowed us to extend our measurements back to shorter times after the quench to the superfluid state, as compared to earlier experiments [1], but we have found no evidence for the expected KZ scenario. Rather than an initially decreasing vortex density, we observe an increasing one. The origin of the vortices detected is attributable to generation through supercritical normal fluid–superfluid counterflow in a second-sound standing wave produced by the expansion. It seems likely that the generation of such a standing wave is inherent to a fast mechanical expansion through the superfluid transition, and that it may in practice set a lower limit to the density of KZ vortices that can be detected by this method. If further improvements of technique enabled reproducible termination of the expansion closer to T_λ and data precision could be improved; however, the substantially reduced vortex growth in the counterflow might still in principle allow the detection of KZ vortices.

ACKNOWLEDGMENTS

We thank Professor L. P. Mezhov-Deglin and Dr. Andrei Ganshyn for useful discussions, and Dr. N. S. Lawson for help with the experiments. This work was supported by the Engineering and Physical Sciences Research Council (U.K.).

[1] M. E. Dodd *et al.*, Phys. Rev. Lett. **81**, 3703 (1998).
[2] T. W. B. Kibble, J. Phys. A **9**, 1387 (1976).
[3] V. L. Ginzburg and L. P. Pitaevskii, Sov. Phys. JETP **7**, 858 (1958).
[4] W. H. Zurek, Nature (London) **317**, 505 (1985).
[5] P. C. Hendry *et al.*, Nature (London) **368**, 315 (1994).
[6] W. H. Zurek, Acta Phys. Pol. B **24**, 1301 (1993).
[7] S. N. Fisher, A. J. Hale, A. M. Guénault, and G. R. Pickett,

Phys. Rev. Lett. **86**, 244 (2001).
[8] M. J. Bowick, L. Chander, E. A. Schiff, and A. M. Srivastava, Science **263**, 943 (1994).
[9] M. J. Bowick, A. Cacciuto, and A. Travesset, J. Low Temp. Phys. **124**, 123 (2001).
[10] R. Monaco, J. Mygind, and R. J. Rivers, Phys. Rev. Lett. **89**, 080603 (2002).
[11] R. Monaco, J. Mygind, and R. J. Rivers, Phys. Rev. B **67**, 104506 (2003).
[12] M. Giltrow *et al.*, Meas. Sci. Technol. **14**, N69 (2003).
[13] L. D. Landau and E. M. Lifshitz, *Fluid Mechanics* (Pergamon Press, Oxford, 1959).
[14] A. Y. Iznankin and L. P. Mezhov-Deglin, Sov. Phys. JETP **57**, 801 (1983).
[15] L. C. Krysac, Phys. Rev. Lett. **73**, 2480 (1994).
[16] V. B. Efimov, G. V. Kolmakov, A. S. Kuliev, and L. P. Mezhov-Deglin, Low Temp. Phys. **24**, 81 (1998).
[17] A. Ganshin, M. Mozzahab, and N. Mulders, J. Low Temp. Phys. **134**, 477 (2004).
[18] P. C. Hendry, N. S. Lawson, and P. V. E. McClintock, J. Low Temp. Phys. **119**, 249 (2000).
[19] C. F. Barenghi and D. C. Samuels, Phys. Rev. Lett. **89**, 155302 (2002).
[20] D. J. Melotte and C. F. Barenghi, Phys. Rev. Lett. **80**, 4181 (1998).
[21] K. W. Schwarz, Phys. Rev. B **31**, 5782 (1985).
[22] K. W. Schwarz, Phys. Rev. B **38**, 2398 (1988).
[23] M. v. Schwerdtner, G. Stamm, and D. W. Schmidt, Phys. Rev. Lett. **63**, 39 (1989).
[24] D. D. Awschalom and K. W. Schwarz, Phys. Rev. Lett. **52**, 49 (1984).
[25] I. M. Khalatnikov, *An Introduction to the Theory of Superfluidity* (Benjamin, New York, 1965).
[26] H. E. Hall and W. F. Vinen, Proc. R. Soc. London, Ser. A **238**, 204 (1956).
[27] H. E. Hall and W. F. Vinen, Proc. R. Soc. London, Ser. A **238**, 215 (1956).
[28] E. B. Sonin, Rev. Mod. Phys. **59**, 87 (1987).
[29] G. E. Volovik, JETP Lett. **78**, 553 (2003).
[30] T. D. C. Bevan *et al.*, J. Low Temp. Phys. **109**, 423 (1997).
[31] A. P. Finne *et al.*, Nature (London) **424**, 1022 (2003).
[32] R. J. Donnelly and C. F. Barenghi, J. Phys. Chem. Ref. Data **27**, 1217 (1998).
[33] R. V. Duncan, G. Ahlers, and V. Steinberg, Phys. Rev. Lett. **60**, 1522 (1988).
[34] A. F. Andreev and L. A. Melnikovsky, JETP Lett. **78**, 574 (2003).
[35] A. F. Andreev and L. A. Melnikovsky, J. Low Temp. Phys. **135**, 411 (2004).
[36] B. N. Eselson *et al.*, *Mixtures of Quantum Liquids* ^{3}He-^{4}He (Nauka, Moscow, 1973).
[37] V. B. Efimov *et al.*, J. Low Temp. Phys. **119**, 309 (2000).